

T. Oberc-Dziedzic · K. Klimas · R. Kryza ·
C. M. Fanning

SHRIMP U–Pb zircon geochronology of the Strzelin gneiss, SW Poland: evidence for a Neoproterozoic thermal event in the Fore-Sudetic Block, Central European Variscides

Received: 6 September 2001 / Accepted: 10 April 2003 / Published online: 11 September 2003
© Springer-Verlag 2003

Abstract Zircon ages recorded in gneissic rocks have recently been used as criteria to define and correlate various tectonic units and crustal blocks in the central European Variscides. A SHRIMP U–Pb zircon geochronological study of the Strzelin gneiss in the Fore-Sudetic Block (SW Poland) indicates the presence of: (1) inherited zircon cores of Palaeo- to Mesoproterozoic ^{206}Pb - ^{238}U ages (between ca. 2,000 and 1,240 Ma), and (2) zoned rims of Neoproterozoic age with two distinct means of 600 ± 7 and 568 ± 7 Ma. The Proterozoic age range of the cores suggests that different Precambrian crustal elements were the source for the protolith of the gneiss. A likely scenario is the erosion of various Proterozoic granites and gneisses, sedimentation (after 1,240 Ma), and partial resistance of the original components to subsequent metamorphic dissolution and/or anatectic resorption (in Neoproterozoic times). The zoned zircon rims of both of the younger Neoproterozoic ages are indistinguishable in the cathodoluminescence images. The data are interpreted in terms of two different thermal events inducing zoned zircon overgrowth at ca. 600 and 568 Ma. In general, the new results confirm earlier assumptions of the Proterozoic age of the gneiss protoliths, and indicate their similarity to orthogneisses in the East Sudetes tectonic domain (e.g. the Velké Vrbno and Desná gneisses). The Neoproterozoic dates are different from the age of 504 ± 3 reported earlier for the Gościęcice gneiss from a neighbouring locality in the Strzelin Massif. The new data strongly indicate a Moravo-Silesian (Bruno-Vistulian) affinity for the Strzelin gneiss and support the

hypothesis that the Strzelin Massif lies within the tectonic boundary zone between the West- and East Sudetes domains, which represents the northern continuation of the Moldanubian Thrust.

Keywords Zircon geochronology · SHRIMP · Gneiss · Neoproterozoic · Strzelin Massif · Fore-Sudetic Block · Sudetes · Moldanubian Thrust · Bohemian Massif · Variscan Belt

Introduction

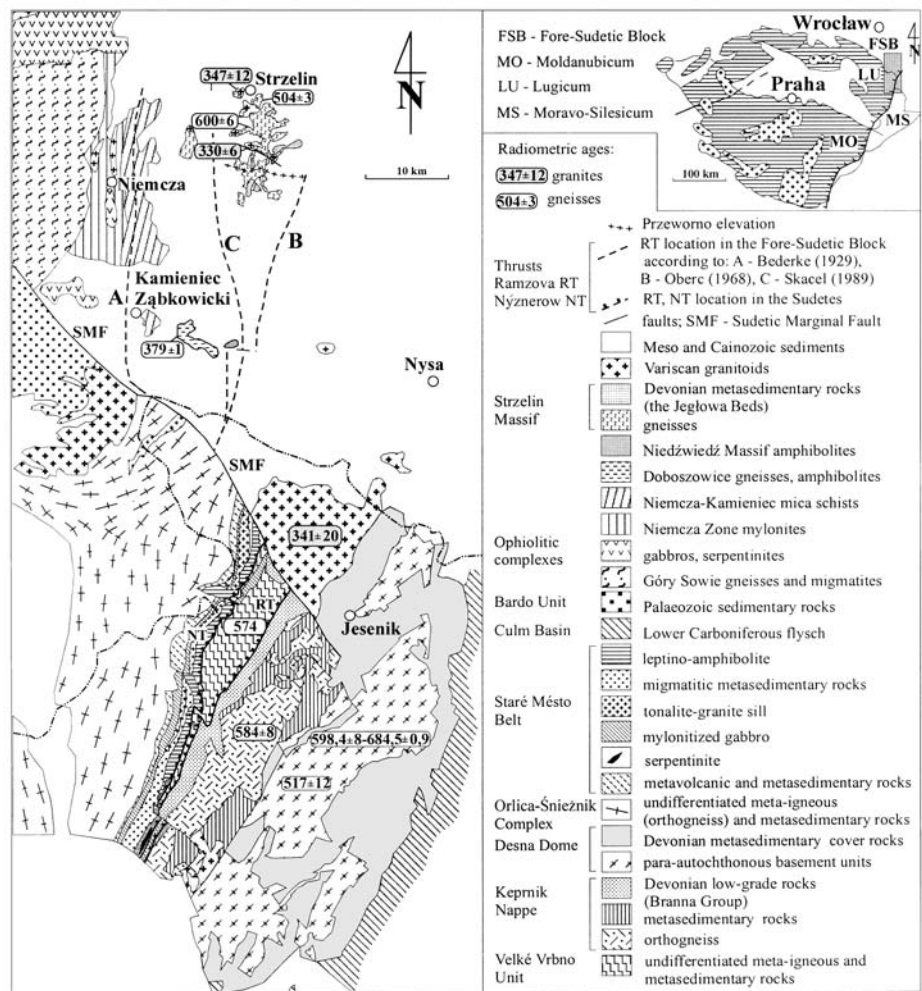
The NE and E part of the Bohemian Massif is a key area for understanding the pre-orogenic and orogenic evolution of the central European Variscides (e.g. Don 1990; Matte et al. 1990; Oliver et al. 1993; Franke et al. 1993; Cymerman et al. 1997; Kröner and Hegner 1998; Aleksandrowski et al. 2000; Collins et al. 2000; Finger et al. 2000; Friedl et al. 2000; Seston et al. 2000; Schulmann and Gayer 2000; Timmermann et al. 2000). This area covers the West and East Sudetes at the Polish/Czech boundary, and the neighbouring Fore-Sudetic Block (FSB) in SW Poland (Fig. 1). The West Sudetes (referred to as Lugicum after Suess 1926; or Sudeticum after Kossmat 1927) display a mosaic structure with a range of tectonic units that have been variously interpreted. Some authors (e.g. Kossmat 1927; Franke et al. 1993) have correlated the West Sudetes with the better defined and more regular, E–W trending major tectonic domains of the Variscan Belt to the west, namely the Saxothuringian Zone (ST) in Germany and in the Czech Republic. Other interpretations of the mosaic structure of the West Sudetes have employed the terrane concept (Matte et al. 1990; Oliver et al. 1993; Cymerman et al. 1997) or emphasized evidence of fragments of a Variscan accretionary prism (Baranowski et al. 1990; Collins et al. 2000).

Along the eastern margin of the Bohemian Massif, the West Sudetes (Lugicum, LU) and the southerly Moldanubicum (MO) are in tectonic contact with a NNE–SSW

T. Oberc-Dziedzic (✉) · K. Klimas · R. Kryza
Institute of Geological Sciences,
University of Wrocław,
pl. M.Borna 9, 50–204 Wrocław, Poland
e-mail: toberc@ing.uni.wroc.pl
Tel.: +48-71-3759449
Fax: +48-71-3759371

C. M. Fanning
Research School of Earth Sciences,
The Australian National University,
0200 Canberra, Australia

Fig. 1 Geological sketch of the border zone between the West and East Sudetes, and the neighbouring part of the Fore-Sudetic Block (compiled on the basis of Puziewicz et al. 1995; Schulmann and Gayer 2000; Oberc et al. 1988, simplified). The *inset map* shows the location of the area within the Bohemian Massif



trending belt, referred to as Moravo-Silesicum (MS; Fig. 1, inset map). This major tectonic boundary had been recognised in the early 20th century by Suess (1912, 1926) who considered it as a large-scale overthrust zone. Recently, Schulmann and Gayer (2000) interpreted the MS as a continental accretionary wedge developed by oblique collision between the MO/LU terrane and the pan-African or “Bruno-Vistulian” microcontinent (Dudek 1980) during the Variscan orogeny.

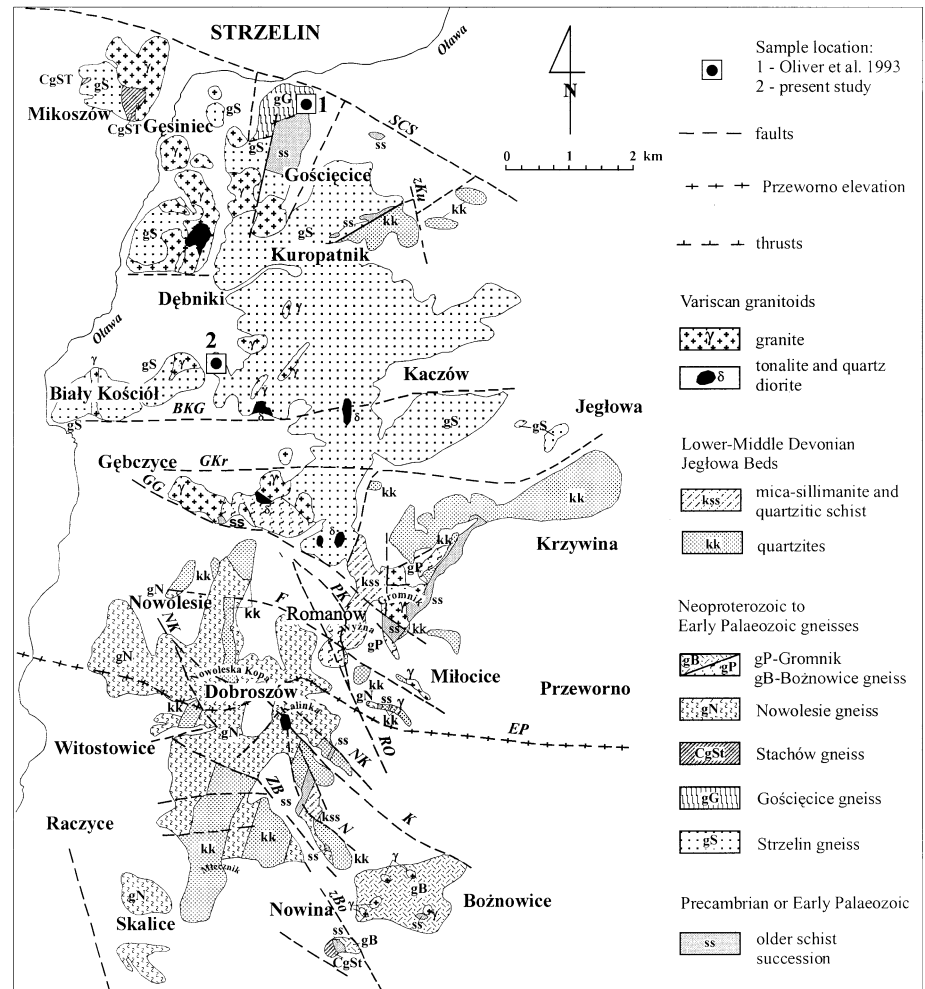
The contact between the MO/LU domains to the west and the MS to the east is well defined in the SE part of the Bohemian Massif (in Moravia), and in the mountainous region of the Sudetes to the north, where it follows, respectively, the Moldanubian Thrust (Suess 1926) and its northern continuation—the Ramzova (and/or Nyznerov) Thrust (Oberc 1957, 1968; Misař 1960; Skácel 1956; Fig. 1). The Ramzova Thrust separates the West Sudetes (Lugicum) from the East Sudetes (northern part of Moravo-Silesicum). Further north, beyond the Sudetic Marginal Fault, i.e. in the poorly exposed area of the Fore-Sudetic Block (Fig. 1), the location of this major tectonic boundary between the Lugicum and Moravo-Silesicum becomes obscure and debatable. Various inter-

pretations place the boundary either along the E edge of the Niemcza Zone (Bederke 1929), or east (Oberc 1968), west (Skácel 1989) or inside the Strzelin Massif (Cwojdzński and Żelaźniewicz 1995; Fig. 1).

Lithostratigraphy, protolith ages, and different P–T–t paths are amongst the criteria used to distinguish between units of MO/LU and MS (Bruno-Vistulicum) affinities and, consequently, to locate the West–East Sudetes boundary. The West Sudetes are characterised by a wide distribution of orthogneisses, with granitic protolith ages of ca. 500 Ma (Oliver et al. 1993). Such gneisses are found for example in the Orlica-Śnieżnik Dome (Fig. 1) and, locally, in the FSB (Gościęcice near Strzelin; Fig. 2). In contrast, the East Sudetes contain abundant orthogneisses of Neoproterozoic ages, e.g. the Keprník gneiss dating from 546 ±6/–8 Ma (van Breemen et al. 1982) and 584±8 Ma (Kröner et al. 2000), the Velké Vrbno gneiss dating from ca. 574 Ma, and the Desná gneiss, dating from between 598.4±0.9 and 684.5±0.9 Ma (Kröner et al. 2000).

This paper presents SHRIMP U–Pb zircon ages for a gneissic rock from the Strzelin Massif (SM) in the eastern part of the FSB, ca. 40 km south of Wrocław (Figs. 1, 2).

Fig. 2 Geological map of the Strzelin Massif (based on Oberc et al. 1988, simplified). Acronyms of names of minor faults are not explained



The new results confirm earlier interpretations of Proterozoic ages for the protolith of the Strzelin gneiss (Oberc 1966). These are surprisingly different from the ages obtained by Oliver et al. (1993) for the Gościęcice gneiss from a neighbouring locality, assumed by those authors to represent the typical Strzelin gneiss. Although the new results do not provide unequivocal evidence for regional correlations, they suggest an affinity of the Strzelin gneiss with the Moravo-Silesicum (Bruno-Visulicum) tectonic domain.

The Strzelin Massif: lithology, structure and metamorphism

The Strzelin Massif (Fig. 2) consists of: (1) Neoproterozoic to Early Palaeozoic gneisses, (2) a Precambrian or Early Palaeozoic older schist succession, and (3) a younger schist succession (Lower–Middle Devonian quartzite and quartzite schist of the Jegłowa Beds) (Oberc-Dziedzic 1995). These three rock units were folded and metamorphosed during Late Devonian–Visian times (Oberc 1966) and subsequently intruded by Variscan granitoids (Oberc-Dziedzic 1995). The relation-

ship of the Strzelin Massif to the other basement units of the FSB remains unclear since the area is largely covered by Cenozoic deposits.

The Neoproterozoic to Early Palaeozoic gneisses comprise four main rock types of various textures and mineral assemblages: (1) fine- to medium-grained, porphyritic biotite-muscovite orthogneisses representing the Strzelin gneiss *sensu stricto* (Fig. 3a); (2) the Gościęcice two-feldspar–biotite augen gneiss (Fig. 3b); (3) the Nowolesie migmatitic, sillimanite gneiss; (4) the Stachów gneiss, represented by two varieties: dark, fine-grained migmatitic gneisses and pale, coarse-grained gneisses. Both the Strzelin gneiss in the northern part of the massif (and its southerly equivalents: the Bożnowice and Gromnik gneisses; Fig. 2), and the Nowolesie gneiss in the southern part of the Strzelin Massif are widespread. The Gościęcice augen gneiss resembles weakly deformed varieties of the Iżera gneisses in the West Sudetes (Oberc-Dziedzic 1988a); it is of limited distribution and has not yet been found in other parts of the FSB. Multi-grain TIMS U–Pb zircon data from the Gościęcice gneiss yielded one concordant zircon fraction at 504 ± 3 Ma (Oliver et al. 1993); two other zircon fractions are discordant, one with a similar $^{207}\text{Pb}/^{206}\text{Pb}$ age of ca.

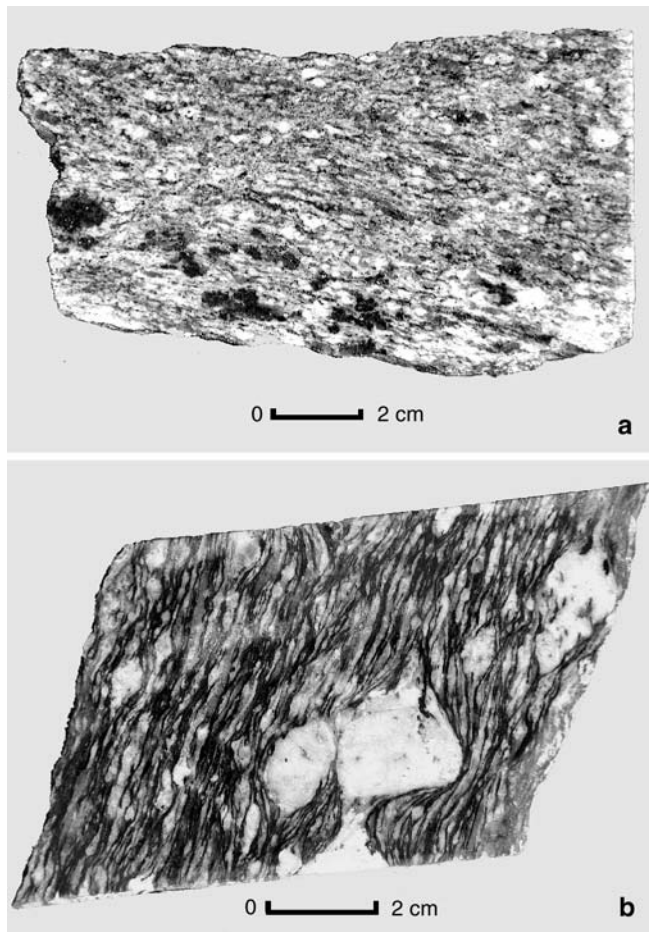


Fig. 3 **a** Sample of the Strzelin gneiss (*sensu stricto*) dated in this study. **b** Gościęcice augen gneiss (referred to as the Strzelin gneiss, *sensu lato*) dated by Oliver et al. (1993) at 504 ± 3 Ma, using the U–Pb multigrain zircon method

500 Ma, the other showing significant inheritance (*op. cit.*).

The older Precambrian or Early Palaeozoic schist succession of amphibolites, mica schists, calc-silicate rocks and marbles is closely connected with the Strzelin gneiss (Fig. 2). In the better-exposed northern part of the Strzelin Massif, the Strzelin gneiss and the rocks of the older schist succession are strongly mylonitised along their contacts. The amphibolites of the older schists succession and those in the Strzelin gneiss are of within-plate tholeiitic character and were interpreted to have been emplaced during an early stage of continental rifting (Szczepański and Oberc-Dziedzic 1998).

The Jęglowa Beds of the younger schist succession (Oberc 1966) consist of quartzites, quartz-sericite schists and metaconglomerates with granitic pebbles (Scheumann 1937). The sedimentation of the Jęglowa Beds was interpreted by Patočka and Szczepański (1997) to have taken place along a continental margin during Early and Mid-Devonian times.

The Variscan granitoids are represented by rocks of various compositions, which were emplaced in succession

from granodiorite, through quartz diorite and tonalite, to biotite granite (347 ± 12 Ma) and biotite-muscovite granite (330 ± 6 Ma; both are Rb–Sr whole-rock ages by Oberc-Dziedzic et al. 1996).

The tectonic structure of the Strzelin Massif was formed during the Variscan orogeny, before the Early Namurian (Oberc-Dziedzic 1999). No evidence of earlier pre-Devonian deformation and metamorphism in the gneisses and in the older schist succession has yet been reported. During the earliest deformation D_1 , the protoliths of the gneisses and older schist succession, and probably part of the Jęglowa beds were folded, metamorphosed and juxtaposed by thrusting. The Gościęcice gneiss was thrust over the amphibolites of the older schist succession and over the Strzelin gneiss. The ca. 10-m-thick thrust zone contains blocks of the HT-HP garnet amphibolites interpreted to have been tectonically transported along the thrust planes. This thrust zone was reactivated during D_3 under greenschist facies conditions (Oberc-Dziedzic 1995, 1999). The direction of thrusting during D_1 is unknown, possibly being top-to-NE or E, similar to the Doboszowice unit, south of the massif (Puziewicz et al. 1995). The oldest fold axes F_1 and the L_1 mineral and intersection lineations generally plunge to the NE in the northern part of the massif and to the SE in its southern part (Wojnar 1995).

The S_1 planar structures were deformed during the D_2 event. The resulting F_2 folds and the L_2 intersection lineation (formed by intersection of the S_1 foliation planes and the S_2 axial cleavage) plunge to the N. In the mica schists, penetrative S_2 planes are parallel to the S_1 foliation. The S_2/S_1 foliation was reactivated during the D_3 deformation event. In the northern part of the Strzelin Massif, the gneisses have an S_3 foliation, mostly parallel to S_2 and S_1 . The S_3 foliation dips to NNE in the northern part of the massif, and to SSW in the southern part. The D_3 deformation induced grain size reduction, the transformation of granitic gneisses into thin-layered gneisses, and a local crenulation of their foliation. Shear-sense indicators generally show an opposing sense of shear: top-to-NE in the northern part, and top-to-SW in the southern part of the Strzelin Massif. The D_4 deformation produced F_4 kink-type folds. The fold axes are WNW–ESE oriented, parallel to the “Przeworno elevation” (Fig. 2; Oberc 1966). The D_4 deformation produced an S_4 foliation in the gneisses, defined as thin mylonitic bands inclined at an angle of 10 – 15° to the S_1/S_3 foliation.

According to Oberc-Dziedzic (1999), the metamorphic conditions during D_1 reached greenschist facies, with temperatures up to ca. 500°C , and various, though moderate, pressures in different parts of the massif. The nappe stacking during the D_1 event gave rise to crustal thickening and, consequently, to an increase in temperature. As a result, the gneisses of the southern part of the SM achieved anatexis conditions after D_1 and before D_2 . The first stage of anatexis was followed by decompression related to the beginning of tectonic denudation, which gave rise to the second stage of anatexis (anatexis melting) and to the subsequent dome-like uplift of the

migmatized rocks. The doming was accompanied by north-eastward and south-westward gravitational collapse, as shown by kinematic indicators (Szczepański 2001).

The final metamorphic episode led to the crystallisation of post-kinematic cordierite and the formation of flecked (spotted) gneisses. Most probably, the cordierite was formed not long before the granitoid emplacement (Oberc-Dziedzic 1988b, 1995), which took place from ca. 350–330 Ma (Oberc-Dziedzic et al. 1996). The deformation structures of these late Variscan tonalites and biotite granites show the same orientation as analogous structures in the adjacent Strzelin Massif gneisses, which suggests that the emplacement of these granitoids took place during the decline of the regional deformation.

Petrography and geochemistry of the Strzelin gneiss

All major types of the gneisses of the Strzelin Massif (Fig. 2) are composed, in various proportions, of quartz, plagioclase, microcline, biotite and muscovite (Fig. 4a, b). The Nowolesie gneiss additionally contains nodules of sillimanite and garnet. The chemical compositions correspond to granite or granodiorite. The Strzelin Massif gneisses are mostly peraluminous and medium to highly potassic (Fig. 4c, d). In spite of their textural diversity, they show many very similar geochemical features: high K, Rb, Ba and Th contents, and positive Ce±Sm and negative Y and Yb anomalies (Szczepański 1999). The chondrite-normalised patterns for the gneisses show flat LREE and enriched HREE distributions, and positive Eu anomalies. Trace-element plots normalised to an average greywacke composition are very flat, which indicates that

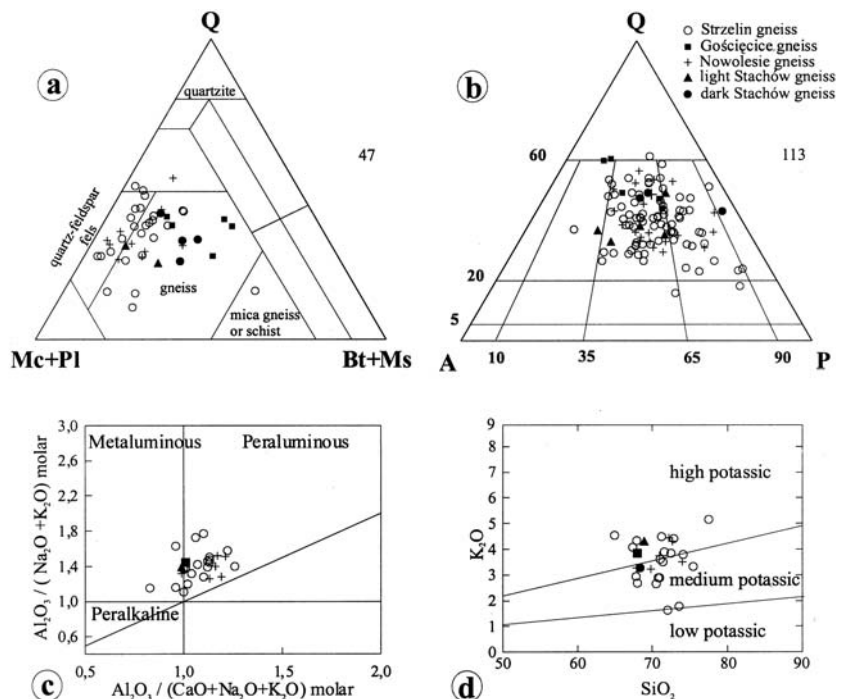
greywacke-type materials were a probable source rock for the protolith of the gneisses (op. cit.). However, the monotonous fabric of the gneisses, their peraluminous character and other geochemical features, as well as the lack of mafic enclaves suggest that an S-type granite could have been an alternative precursor for the gneisses.

The sample selected for U–Pb zircon geochronology is a Strzelin gneiss from the exposure near the village of Dębniaki (Figs. 2, 3a). The sample represents the most typical and widespread variety of the Strzelin gneiss (*sensu stricto*). The gneiss is a light-grey, medium-grained, porphyritic rock, with a weak foliation and lineation. The foliation is defined by aligned multi-grain quartz aggregates and biotite streaks. The matrix is composed of two generations of plagioclase (An₂₂ and An₁₂), microcline, quartz, biotite and muscovite. Plagioclase and microcline form porphyroblasts (megacrysts?) up to 0,5 mm in size, with inclusions of coarse-grained muscovite and concave quartz grains. Reddish-brown biotite with pleochroic halos around scarce zircon grains are locally associated with sillimanite clusters. Sillimanite needles and euhedral zircon grains occur as inclusions in plagioclase and quartz. Dark-coloured mica pseudomorphs after cordierite (up to 1 cm in size) overgrow the foliation.

Analytical techniques

A jaw crusher was used to break down the sample to a grain size of <300 µm. Heavy mineral concentrates were separated using conventional sieving, heavy-liquid and paramagnetic techniques. Zircons were handpicked under a binocular microscope from the ore-free concentrate,

Fig. 4 The gneisses of the Strzelin Massif: **a** mineral composition (47 samples); **b** QAP diagram (113 samples); **c** Shand (1947) classification (28 samples); **d** K₂O–SiO₂ diagram (28 samples)



mounted in epoxy together with the AS3 Duluth Gabbro reference zircon, sectioned approximately in half and polished. Transmitted and reflected light photomicrographs and cathodoluminescence (CL) images were made for all zircons. The U–Pb analyses of 11 zircon grains (core and rim pairs) were determined using the Sensitive High Resolution Ion Microprobe (SHRIMP II) at The Australian National University; each analysis consisting of six scans through the mass spectrum. The analyses and data reduction have been carried out using standard procedures as described in Williams (1998, and references therein). The Pb/U ratios have been normalised relative to a value of 0.1,859 for the $^{206}\text{Pb}/^{238}\text{U}$ ratio of the AS3 reference zircons, equivalent to an age of 1,099 Ma (see Paces and Miller 1993). Uncertainties given for individual analyses (ratios and ages) are at the 1σ level, however the uncertainties in calculated weighted mean ages are reported as 95% confidence limits. Tera and Wasserburg (1972) concordia plots and weighted mean $^{206}\text{Pb}/^{238}\text{U}$ ages were carried out using ISOPLOT/EX (Ludwig 1999).

Results

The zircons selected for analysis are dominantly colourless, clear prismatic grains with bipyramidal terminations. Under transmitted light, only a few of these grains show internal structure, though there are others in the wider population that have abundant opaque and other inclusions, or are broken or have internal cracks. For the hand-selected, optically clear grains, the CL imaging reveals the true internal structure and complexity of these zircons (Fig. 5). The simple fact that such apparently optically homogeneous grains have complex internal structure highlights the necessity for such CL imaging prior to any U–Pb analysis (e.g. Hanchar and Miller 1993; Vavra et al. 1996; Rubatto and Gebauer 2000). Nearly every grain comprises a structurally discordant central area, overgrown by an oscillatory-zoned rim. The latter gives rise to the observed prismatic external morphology of the grains with bipyramidal terminations, and is interpreted to represent zircon growth from a melt.

The central or core areas can be subdivided into two types: one that is poorly structured, for example grains 4, 7, 9 and 11 (and perhaps the weakly zoned core of grain 3), and another which shows simple zonation, for example grains 1, 2, 5, 6, 8 and 10. The poorly structured cores are often interpreted to be metamorphic in origin, whereas the zoned areas as more clearly derived from a magmatic precursor. This interpretation, however, remains controversial (cf. Rubatto and Gebauer 2000; Kempe et al. 2000, and references therein).

Analyses of these central areas record a range in ages from the Palaeoproterozoic through to the Neoproterozoic, the latter being close to those of the rim ages (grains 5, 6 and 9). Analysis 11.1 is of an area that is part of a low U (light CL), poorly structured, probably metamorphic

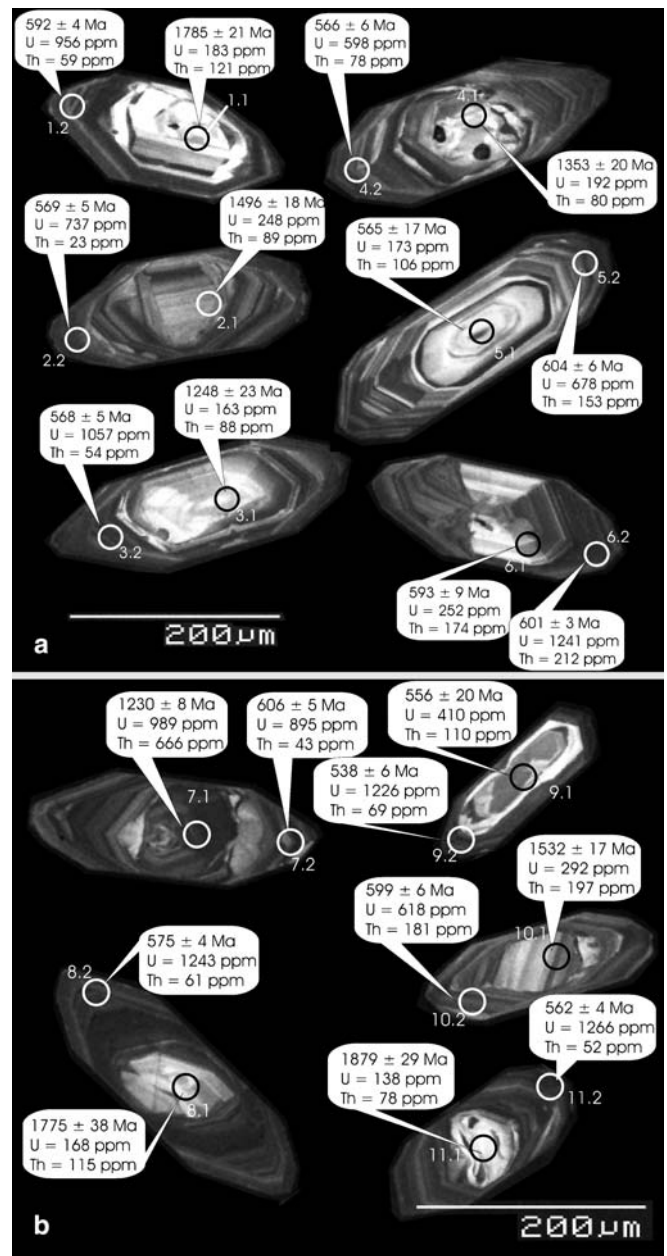


Fig. 5 **a** Cathodoluminescence images of the zircon grains analysed from the Strzelin gneiss; grain 4 has a poorly structured core whereas the cores in the remaining zircons in this figure display distinct zonation. The circles indicate spots analysed, and the labels give the $^{206}\text{Pb}/^{238}\text{U}$ ages. **b** Cathodoluminescence images of the zircon grains analysed from the Strzelin gneiss (continued); the cores of grains 7, 9 and 11 are poorly structured, and those in grains 8 and 10 have simple zonation

core, recording the oldest $^{207}\text{Pb}/^{206}\text{Pb}$ age of ca. 2,000 Ma (Table 1 and Fig. 6). Both the magmatic and metamorphic cores, as interpreted, record Proterozoic $^{207}\text{Pb}/^{206}\text{Pb}$ ages between ca. 2,000 and 1,240 Ma (analysis 7.1). The presence of heterogeneous inherited cores, together with the range in inherited ages, indicates that the protolith to this gneissic rock was most probably sedimentary. It is common for such zircons to survive melting of the

Table 1 Summary of SHRIMP U-Pb zircon results for Strzelin gneiss sample

Grain spot	U (ppm)	Th (ppm)	Th/U	Pb* (ppm)	$\frac{^{204}\text{Pb}}{^{206}\text{Pb}}$	f_{206} (%)	Total ratios		Radiogenic ratios		Ages (Ma)		Conc. (%)										
							$\frac{^{206}\text{Pb}}{^{238}\text{U}}$	$\frac{^{207}\text{Pb}}{^{206}\text{Pb}}$	\pm	$\frac{^{206}\text{Pb}}{^{238}\text{U}}$	\pm	$\frac{^{207}\text{Pb}}{^{235}\text{U}}$		\pm	$\frac{^{207}\text{Pb}}{^{206}\text{Pb}}$	\pm							
1.1	183	121	0.66	62	0.000041	0.06	3.132	0.041	0.1114	0.0007	0.3191	0.0042	4.877	0.076	0.111	0.0008	1.785	21	1,798	13	1.813	13	98
1.2	956	59	0.06	80	0.000052	<0.01	10.410	0.076	0.0611	0.0004	0.0961	0.0007	0.0007	0.0000	0.0000	0.0000	592	4	1,495	15	1,495	23	100
2.1	248	89	0.36	62	0.000162	0.26	3.819	0.051	0.0956	0.0010	0.2611	0.0035	3.360	0.065	0.093	0.0011	1,496	18	1,495	15	1,495	23	100
2.2	737	23	0.03	59	0.000113	0.04	10.838	0.094	0.0647	0.0006	0.0922	0.0008	0.0008	0.0000	0.0000	0.0000	569	5	1,268	17	1,301	19	96
3.1	163	88	0.54	35	0.000022	0.04	4.680	0.095	0.0847	0.0008	0.2136	0.0044	2.485	0.059	0.084	0.0008	1,248	23	1,268	17	1,301	19	96
3.2	1057	54	0.05	84	0.000053	<0.01	10.852	0.092	0.0607	0.0004	0.0922	0.0008	0.0008	0.0000	0.0000	0.0000	568	5	1,347	20	1,338	36	101
4.1	192	80	0.42	43	0.000152	0.24	4.270	0.070	0.0881	0.0010	0.2336	0.0038	2.769	0.072	0.086	0.0016	1,353	20	1,347	20	1,338	36	101
4.2	598	78	0.13	49	0.000066	0.1	10.882	0.118	0.0615	0.0006	0.0918	0.0010	0.0010	0.0000	0.0000	0.0000	566	6					
5.1	173	106	0.61	16	0.000230	0.36	10.869	0.336	0.0637	0.0011	0.0917	0.0028	0.0028	0.0000	0.0000	0.0000	565	17					
5.2	678	153	0.23	61	0.000096	<0.01	10.197	0.098	0.0607	0.0005	0.0982	0.0010	0.0010	0.0000	0.0000	0.0000	604	6					
5.3	252	174	0.69	25	0.000564	0.24	10.357	0.161	0.0636	0.0010	0.0963	0.0015	0.0015	0.0000	0.0000	0.0000	593	9					
6.1	1241	212	0.17	109	0.000083	<0.01	10.241	0.060	0.0604	0.0004	0.0978	0.0006	0.0006	0.0000	0.0000	0.0000	601	3					
6.2	989	666	0.67	214	0.000031	0.05	4.754	0.035	0.0823	0.0004	0.2102	0.0016	2.373	0.023	0.082	0.0004	1,230	8	1,235	7	1,242	10	99
7.1	895	43	0.05	77	0.000027	<0.01	10.154	0.090	0.0602	0.0006	0.0987	0.0009	0.0009	0.0000	0.0000	0.0000	606	5					
7.2	168	115	0.68	56	0.000111	0.17	3.150	0.078	0.1095	0.0009	0.3169	0.0078	4.720	0.130	0.108	0.0010	1,775	38	1,771	23	1,766	18	101
8.1	1243	61	0.05	101	0.000077	<0.01	10.719	0.077	0.0603	0.0005	0.0933	0.0007	0.0007	0.0000	0.0000	0.0000	575	4					
8.2	410	110	0.27	34	0.000441	0.38	11.060	0.411	0.0638	0.0013	0.0901	0.0034	0.0034	0.0000	0.0000	0.0000	556	20					
9.1	410	110	0.27	34	0.000441	0.38	11.060	0.411	0.0638	0.0013	0.0901	0.0034	0.0034	0.0000	0.0000	0.0000	556	20					
9.2	1226	69	0.06	93	0.000202	<0.01	11.494	0.122	0.046	0.0006	0.0871	0.0009	3.459	0.060	0.093	0.0010	1,532	17	1,518	14	1,498	20	102
10.1	292	197	0.67	81	0.000075	0.12	3.722	0.046	0.0945	0.0007	0.2684	0.0034	3.459	0.060	0.093	0.0010	1,532	17	1,518	14	1,498	20	102
10.2	618	181	0.29	56	0.000064	<0.01	10.277	0.110	0.0608	0.0006	0.0974	0.0011	0.0011	0.0000	0.0000	0.0000	599	6					
11.1	138	78	0.56	48	0.000151	0.23	2.948	0.052	0.1252	0.0010	0.3384	0.0060	5.749	0.124	0.123	0.0013	1,879	29	1,939	19	2,003	19	94
11.2	1266	52	0.04	100	0.000208	0.11	10.964	0.071	0.0617	0.0004	0.0911	0.0006	0.0006	0.0000	0.0000	0.0000	562	4					

Uncertainties given at the 1σ level. Error in the AS3 reference zircon was 0.92% at 95% CI for this analytical session; f_{206} % denotes the percentage of ^{206}Pb that is common Pb; For areas >800 Ma, correction for common Pb was made using the measured $^{204}\text{Pb}/^{206}\text{Pb}$ ratio; For areas <800 Ma, correction for common Pb was made using the measured ^{207}Pb correction method (Williams 1998, and references therein). Necessarily for such analyses, it is not possible to present radiogenic ratios or ages using ^{207}Pb ; For Conc. (%), 100% denotes a concordant analysis

surrounding rock and subsequent crystallisation within a granitic melt (e.g. Williams 2000).

Analyses of the zoned magmatic rims surprisingly do not define a simple age pattern, as can be seen on an enlarged Tera-Wasserburg concordia plot (Fig. 6, inset). Rather there appears to be a range in ages recorded that is best examined on a cumulative probability plot, with a stacked histogram. This plot shows two quite distinct age peaks with a minor peak trailing off at the younger end of the age spectrum (Fig. 7). Prior to discussing this prominent bimodal age pattern, it is necessary to discuss the analyses of grains 5, 6 and 9. Grain 9 is relatively small and comprises a central component containing ca. 410 ppm U, surrounded by a thin rim containing ca. 1,230 ppm U, that is relatively structureless. Analysis 9.1 of the core is poorly constrained and contains significant common Pb (Fig. 6), whereas rim analysis 9.2 yielded the youngest $^{206}\text{Pb}/^{238}\text{U}$ age of ca. 540 Ma. The latter area is interpreted to have lost significant amounts of radiogenic Pb and plots on a simple Pb loss trend towards the present day on the Tera-Wasserburg concordia plot (Fig. 6). The core analysis 9.1 has a high degree of uncertainty and it is possible that even on the scale of the ca. 20 μm SHRIMP spot the analysis was of an area of heterogeneous zircon. Neither of these two analyses is considered to yield geologically meaningful data and so they are not considered further.

For grains 5 and 6, analyses of the central areas appear to be younger than the rim analyses. Analysis of the core to grain 5 (analysis 5.1) is poorly constrained ($^{206}\text{Pb}/^{238}\text{U}$ age = 565 ± 17 Ma, 1 sigma uncertainty); no cracks are visible through which the zircon could have lost radiogenic Pb, but the analysed area is slightly clouded by very fine inclusions, which indicates a possible compositional disturbance. Analysis 6.1 is of the zoned central part of grain 6. It has a $^{206}\text{Pb}/^{238}\text{U}$ age of 593 ± 9 Ma (1 sigma uncertainty) that is within analytical uncertainty of the rim analysis 6.2 at 601 ± 3 Ma (1σ uncertainty). We therefore interpret grain 6 as having wholly formed during a single magmatic event, resulting in continuous, simple igneous zonation from core to rim.

The remaining analyses are all of zoned magmatic rims and on a relative probability plot form two distinct groupings of $^{206}\text{Pb}/^{238}\text{U}$ ages (Fig. 7). Analyses 1.2, 5.2, 6.2, 7.2 and 10.2, together with analysis 6.1 discussed above, have a weighted mean $^{206}\text{Pb}/^{238}\text{U}$ age of 600 ± 7 Ma (95% confidence limits). In contrast, analyses 2.2, 3.2, 4.2, 8.2 and 11.2 have a weighted mean $^{206}\text{Pb}/^{238}\text{U}$ age of 568 ± 7 Ma (95% confidence limits). There is no unique relationship between these two respective age groupings and the U, Th, or Th/U ratios of the areas analysed, although the younger group tends to have lower Th (all <80 ppm) and Th/U ratios (all <0.13) than the older group. In the older group, analyses 1.2 and 7.2 have low Th and low Th/U ratios. The other four analyses have Th/U ratios greater than 0.15 to 0.2, which is normally considered to reflect magmatic paragenesis (e.g. Rubatto and Gebauer 2000).

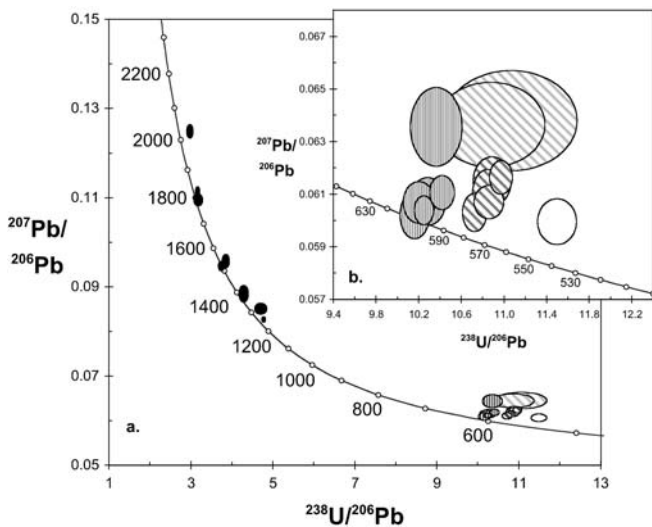


Fig. 6 Tera and Wasserburg (1972) concordia plot of SHRIMP analyses for the Strzelin gneiss showing the total $^{207}\text{Pb}/^{206}\text{Pb}$ ratios vs. the calibrated $^{238}\text{U}/^{206}\text{Pb}$ ratios, uncorrected for common Pb; analyses are plotted as 1 sigma error ellipses. Inset shows an enlarged view of the Neoproterozoic zircon analyses

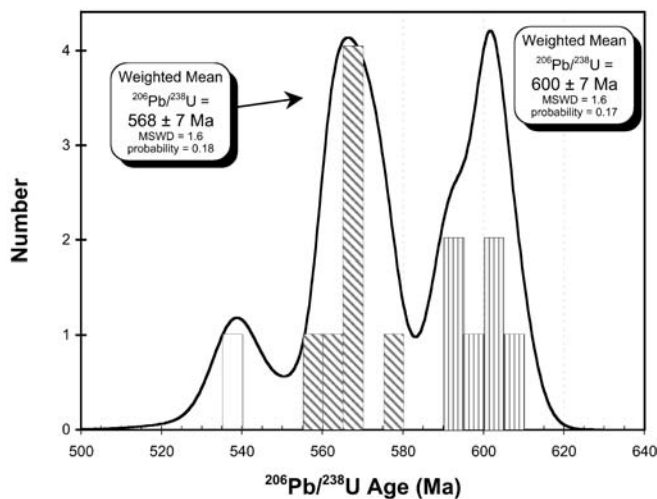


Fig. 7 Cumulative probability plot, with stacked histogram (using Ludwig 1999) of the radiogenic $^{206}\text{Pb}/^{238}\text{U}$ ages for the Neoproterozoic age zircon analyses from the Strzelin gneiss. Weighted mean $^{206}\text{Pb}/^{238}\text{U}$ age calculations for the two prominent peaks are included

Discussion

Timing of events

Inherited zircon components are prominent in the zircons analysed from the Strzelin gneiss, as clearly seen in the CL images. The inheritance is dated by Proterozoic $^{207}\text{Pb}/^{206}\text{Pb}$ ages ranging between ca. 2,000 and 1,240 Ma. This range of inherited ages indicates that several different Precambrian crustal elements sourced the Strzelin gneiss. We therefore propose that the original protoliths of the

Strzelin gneiss were sedimentary rocks derived from the erosion of continental crust containing granites and/or gneisses of various Proterozoic ages. This conclusion is in accord with the petrographic and geochemical characteristics of the Strzelin gneiss (see above).

The analyses of the zoned rims appear to form two age groupings, one at 600 ± 7 Ma, and the other at 568 ± 7 Ma. The two age groupings cannot be distinguished on morphological grounds or by CL imaging. Zircons of the younger age group tend to have lower Th contents and lower Th/U ratios, but there is a significant overlap with zircons of the older age group.

The older group is considered to have U and Th contents that are consistent with a normal igneous paragenesis (cf. Rubatto and Gebauer 2000; Kempe et al. 2000, and references therein), whereas the younger group may have resulted from crystallisation during a later partial melting associated with metamorphism. However, in the 11 grains analysed, there is no conclusive evidence for 570 Ma outer rims overgrowing 600 Ma inner rims/cores; thus the question whether we are dealing with distinct two zircon-crystallization events needs testing by more analyses.

The protolith of the Strzelin gneiss was subsequently affected by Late Devonian–Early Carboniferous deformation and metamorphism which ceased before the emplacement of the Variscan two-mica granites at ca. 330 Ma (Oberc-Dziedzic 1999). This obliterated original features of the Neoproterozoic precursors of the gneiss but the zircons studied so far do not document Variscan events.

Regional correlations

Friedl et al. (2000) reported SHRIMP analyses of inherited zircons of ca. 1,65–1,8, 1.5, and 1.2 Ga, in the Biteš gneisses from the southern part of Moravo-Silesicum, and thus provided evidence for Mesoproterozoic and late Paleoproterozoic thermal events in this area. They considered their findings “as a strong argument in favour of a South American derivation of the Moravo-Silesian unit and for its affiliation to Avalonia”. The Strzelin gneiss contains inherited zircons of very similar ages, which supports the Moravo-Silesian affinity of the Strzelin gneiss and its possible connection to Avalonia.

The age of 504 ± 3 Ma by Oliver et al. (1993) for the Gościęcice gneiss from the vicinity of Strzelin (Figs. 2, 3b) was assumed by these authors to be representative for all the gneisses of the Strzelin Massif, although the sample comprised a minor and atypical variety of the gneisses found in that area. On this basis, the Strzelin gneisses (sensu lato), together with several other Cambrian/Ordovician orthogneisses from different parts of the Sudetic mosaic, were included into the “Sudetan batholith” terrane (Oliver et al. 1993). Our results, with two means of 600 ± 7 and 568 ± 7 Ma, show that the protolith of the Strzelin gneiss (sensu stricto; Fig. 3a) is older than that of the Gościęcice gneiss. It is now evident that these

two varieties of the gneisses from the Strzelin Massif differ not only in fabric but also in age.

The Neoproterozoic ages of the Strzelin gneiss protolith indicate its affinity to the East Sudetes tectonic domain, and support the earlier hypothesis of Bederke (1929, 1931) and Oberc (1966), who compared the Strzelin gneisses with similar rocks in Moravo-Silesicum. All of the orthogneisses of the East Sudetes domain have Neoproterozoic ages. The Keprnik gneiss, previously dated at 546 ± 6 Ma by the U–Pb method, and at 550 Ma by the Rb/Sr method (both ages by van Breemen et al. 1982), was recently analysed by the vapour digestion technique (Kröner et al. 2000) providing a concordia intercept age of 584 ± 8 Ma. The $^{207}\text{Pb}/^{206}\text{Pb}$ zircon protolith ages are ca. 574 Ma for the Velké Vrbno orthogneiss, and between 598.4 ± 0.9 and 684.5 ± 0.9 Ma for the Desná gneiss (Kröner et al. 2000). The Cambro-Ordovician magmatic activity affecting the Moravo-Silesian Cadomian basement is documented by granitic (517 ± 12 Ma) and pegmatitic dykes (502.3 ± 1 Ma) cross-cutting the 684-Ma gneiss and 506.7 ± 1.7 -Ma migmatite, respectively (op. cit.). In addition to their similar protolith ages, the Strzelin orthogneiss and the Keprnik orthogneiss are geochemically similar, and resemble high-K granitoids of the western part of Bruno-Vistulicum further southwards. The latter were interpreted as mainly crustal-derived rocks with cratonic components involved in the melting processes (Finger et al. 2000; Kröner et al. 2000).

The relationships between the Neoproterozoic gneisses and the Cambro-Ordovician granites or their metamorphic equivalents, reported locally as evidently intrusive in Moravo-Silesicum (see above), appear to be obscured by tectonic processes in the Strzelin Massif, where e.g. the Cambro-Ordovician Gościęcice gneiss is thrust over the Neoproterozoic Strzelin gneiss (*sensu stricto*) and its metamorphic cover (Oberc-Dziedzic and Szczepański 1995). The ca. 10-m-thick thrust zone contains fragments of relatively HT-HP garnet amphibolite tectonically transported along the fault (Oberc-Dziedzic 1995, 1999). Similar relationships between gneisses of different ages were observed along the Moldanubian Thrust (Suess 1926) and along its northern continuation—the Ramzova/Nyznerov Thrust (Bederke 1929; Oberc 1957; Misař 1960; Skacel 1956), where the Early Palaeozoic orthogneisses (e.g. the Gföln and Śnieżnik orthogneisses) are thrust eastwards over Cadomian (Moravo-Silesian) basement. Thus, it is likely that the thrust separating the Gościęcice gneiss from the Strzelin gneiss represents part of the tectonic boundary between the West- and East Sudetes tectonic domains.

The East Sudetes tectonic domain (Fig. 1), comprising the Keprnik biotite orthogneiss, the Velké Vrbno tonalitic orthogneiss, and the Desná gneiss, was interpreted as part of the Cadomian (Pan-African) Bruno-Vistulian microcontinent (Dudek 1980), dismembered during Devonian–Carboniferous tectonic events (Schulmann and Gayer 2000; Kröner et al. 2000). The strong evidence for the East Sudetes affinity of the Strzelin gneiss indicates that a similar interpretation is justified also for the Strzelin

Massif. Consequently, fragments of Neoproterozoic Bruno-Vistulicum basement can be traced further north, beyond the mountainous East Sudetes region, in the eastern part of the Fore-Sudetic Block. The new results combined with structural observations also indicate that the Strzelin Massif can be located within the major tectonic zone separating the West Sudetes and Moravo-Silesicum (i.e. within the northern continuation of the Moldanubian Thrust), the precise location of which within the poorly exposed Fore-Sudetic Block has remained a matter of debate since the work of Bederke (1929).

Acknowledgements This study was supported by internal grants 1017/S/ING/00/III, 2022/W/ING/00/17 and 2022/W/ING/00/21 from the University of Wrocław. Maciej Kryza and Stanisław Madej helped to prepare computerised versions of the CL images and photos of the samples, respectively. The valuable review by Fritz Finger and detailed comments by Hilke Timmermann are acknowledged. Jan Zalasiewicz is thanked for his improvements and English corrections.

References

- Aleksandrowski P, Kryza R, Mazur S, Pin C, Zalasiewicz JA (2000) The Polish Sudetes: Caledonian or Variscan? *Trans R Soc Edinb: Earth Sci* 90:127–146
- Baranowski Z, Haydukiewicz A, Kryza R, Lorenc S, Muszyński A, Solecki A, Urbanek Z (1990) Outline of the geology of the Góry Kaczawskie (Sudetes, Poland). *Neues Jahrb Geol Paläontol Abh* 179:223–257
- Bederke E (1929) Die Grenze von Ost- und Westsudeten und ihre Bedeutung für die Einordnung der Sudeten in den Gebirgsbau Mitteleuropas. *Geol Rundsch* 20:186–205
- Bederke E (1931) Die moldanubische Überschiebung im Sudeten-vorlande. *Zentralb Mineral Geol Paläontol Abteilungen B*: 349–408
- Collins AS, Kryza R, Zalasiewicz J (2000) Microfabric fingerprints of Late Devonian–Early Carboniferous subduction in the Polish Variscides, the Kaczawa Complex, Sudetes. *J Geol Soc Lond* 157:283–288
- Cwojdzinski S, Żelaźniewicz A (1995) Crystalline basement of the Fore-Sudetic Block. Guide to excursions (in Polish with English summary). LXVI Annual Meeting of Polish Geological Society, *Ann Soc Geol Poloniae*, pp 11–126
- Cymerman Z, Piasecki MA, Seston R (1997) Terranes and terrane boundaries in the Sudetes, northeast Bohemian Massif. *Geol Mag* 134:717–725
- Don J (1990) The differences in Paleozoic facies—structural evolution of the West Sudetes. *Neues Jahrb Geol Paläontol Abh* 179:307–328
- Dudek A (1980) The crystalline basement block of the outer Carpathians in Moravia-Brunovistulicum. *Rozprawy Česk Akad Véd, Rada Mate Přírodních Véd* 90:1–85
- Finger F, Hanzl P, Pin C, von Quadt A, Steyer HP (2000) The Brunovistulian: Avalonian Precambrian sequence at the eastern end of the Central European Variscides? In: Franke W et al. (eds) *Orogenic processes: Quantification and modelling in the Variscan Belt*. *Geol Soc Spec Publ* 179:103–112
- Franke W, Żelaźniewicz A, Porebski SJ, Wajsprych B (1993) Saxothuringian zone in Germany and Poland: differences and common features. *Geol Rundsch* 82:583–599
- Friedl G, Finger F, McNaughton NJ, Fletcher IR (2000) Deducing the ancestry of terranes: SHRIMP evidence for South America-derived Gondwana fragments in central Europe. *Geology* 28:1035–1038

- Hanchar JM, Miller CF (1993) Zircon zonation patterns as revealed by cathodoluminescence and backscattered electron images: implications for interpretation of complex crustal histories. *Chem Geol* 110:1–13
- Hanžl P, Mazur S, Melichar R, Buriankova K (1998) Geochemistry of the Doboszowice orthogneiss and its correlation with rocks of the Silesicum and Moravicum. *Polsk Towarzystwo Mineral—Prace Specj* 11:100–103
- Kempe U, Gruner T, Nasdala L, Wolf D (2000) Relevance of cathodoluminescence for the interpretation of U–Pb zircon ages, with an example of an application to a study of zircons from the Saxonian Granulite Complex, Germany. In: Pagel M, Barbin V, Blanc P, Ohnenstetter D (eds) *Cathodoluminescence in geosciences*. Springer, Berlin Heidelberg New York pp 415–455
- Kossmat F (1927) Gliederung des varistischen Gebirgsbaues. *Abh Sächsischen Geol Landesamts* 1:1–39
- Kröner A, Hegner E (1998) Geochemistry, single zircon ages, and Sm–Nd systematics of granitoid rocks from the Góry Sowie (Owl Mts.), Polish West Sudetes: evidence for early Paleozoic arc-related plutonism. *J Geol Soc Lond* 155:711–724
- Kröner A, Štípska P, Schulmann K, Jaeckel P (2000) Chronological constraints on the pre-Variscan evolution of the northeastern margin of the Bohemian Massif, Czech Republic. In: Franke W et al. (eds) *Orogenic processes: quantification and modelling in the Variscan Belt*. *Geol Soc Lond Spec Publ* 179 pp 175–197
- Ludwig KR (1999) User's manual for Isoplot/Ex, Version 2.10, A geochronological toolkit for Microsoft Excel. Berkeley Geochronology Center Special Publication No. 1a, 2455 Ridge Road, Berkeley CA 94709, USA
- Matte P, Maluski H, Reilich P, Franke W (1990) Terrane boundaries in the Bohemian Massif: results of large scale Variscan shearing. *Tectonophysics* 177:151–170
- Mazur S, Puziewicz J, Szczepański J (1997) Deformed granites from Lipniki (Fore-Sudetic Block): record of Variscan extension in the west/East Sudetes boundary zone (SW Poland) (in Polish with English summary). *Przegląd Geol* 45:290–294
- Misar Z (1960) Abermals über die geologische Grenze zwischen den Ost- und Westsudeten und über die sogenannte moldanubische Überschiebung in diesem Gebiet. *Neues Jahrb Miner Monatsh* 4:148–180
- Oberc J (1957) Directions of orogenic stresses in the border zone of Eastern and Western Sudeten (in Polish with English summary). *Acta Geol Polon* 7:1–27
- Oberc J (1966) Geology of crystalline rocks of the Wzgórza Strzelińskie Hills, Lower Silesia (in Polish with English summary). *Studia Geol Polonica* 20:1–187
- Oberc J (1968) The boundary between the western and eastern sudetic tectonic structure (in Polish with English summary). *Rocznik Polsk Towarzystwa Geol* 38:203–271
- Oberc J (ed), Oberc-Dziedzic T, Klimas-August K (eds) (1988) *Mapa geologiczna Wzgórz Strzelińskich w skali 1:25 000*. Instytut Nauk Geologicznych Uniwersytetu Wrocławskiego, Przedsiębiorstwo Geologiczne Wrocław
- Oberc-Dziedzic T (1988a) Serie metamorficzne Wzgórz Strzelińskich i historia ich przeobrażeń. *Materiały do sesji naukowej: Budowa, rozwój i surowce skalne krystaliniku strzelińskiego* (in Polish). Instytut Nauk Geologicznych Uniwersytetu Wrocławskiego, Przedsiębiorstwo Geol Wrocław: 6–21
- Oberc-Dziedzic T (1988b) Genese des gneiss fétaches de cordiérite dans les roches cristallines de Wzgórz Strzelińskie. In: Lorenc S, Majerowicz A (eds) *Petrologia i geologia fundamentu wartyjskiego polskiej części Sudetów: wyniki współpracy naukowej między Uniwersytetem Wrocławskim i Uniwersytetem Clermont-Ferrand*: 63–73
- Oberc-Dziedzic T (1995) Research problems of the Wzgórz Strzelińskie metamorphic series in the light of the analysis of borehole materials (in Polish with English summary). *Acta Universitatis Wratislaviensis* 1739, *Prace Geol-Mineral* 50:75–105
- Oberc-Dziedzic T (1999) The metamorphic and structural development of gneisses and older schist series in the Strzelin crystalline massif (Fore-Sudetic Block, SW Poland). *Mineral Soc Poland Spec Pap* 14:10–21
- Oberc-Dziedzic T, Pin C, Duthou JL, Couturie JP (1996) Age and origin of the Strzelin granitoids (Fore-Sudetic Block, Poland): $^{87}\text{Rb}/^{86}\text{Sr}$ data. *Neues Jahrb Mineral Abh* 171:187–198
- Oberc-Dziedzic T, Szczepański J (1995) Geology of the Wzgórza Strzelińskie crystalline massif (in Polish with English summary). Guide to excursions LXVI Annual Meeting of Polish Geological Society. *Ann Soc Geol Polon* pp 111–126
- Oliver GJH, Corfu F, Krough TE (1993) U–Pb ages from SW Poland: evidence for a Caledonian suture zone between Baltica and Gondwana. *J Geol Soc Lond* 150:355–369
- Paces JB, Miller JD (1993) Precise U–Pb ages of Duluth Complex and related mafic intrusions, northeastern Minnesota: Geochronological insights to physical, petrogenetic, paleomagnetic, and tectonomagmatic process associated with the 1.1 Ga Midcontinent Rift System. *J Geophys Res* 98:13997–14013
- Patočka F, Szczepański J (1997) Geochemistry of quartzites from the eastern margin of the Bohemian Massif (the Hrubý Jeseník Mts. Devonian and the Strzelin crystalline massif): provenance and tectonic setting of deposition. *Polsk Towarzystwo Mineral—Prace Specjalne* 9:151–154
- Puziewicz J, Mazur S, Papiewska C (1995) Petrography and origin of two-mica paragneisses and amphibolites of the Doboszowice metamorphic unit (Sudetes, SW Poland) (in Polish with English summary). *Arch Mineral* 52:35–70
- Rubatto D, Gebauer D (2000) Use of cathodoluminescence for U–Pb zircon dating by ion microprobe: some examples from the Western Alps. In: Pagel M, Barbin V, Blanc P, Ohnenstetter D (eds) *Cathodoluminescence in geosciences*. Springer, Berlin Heidelberg New York, pp 373–400
- Scheumann KH (1937) *Sudetische Studien III. Konglomerattektonite und ihre Begleitgesteine in der epizonalen Schiefer-scholle südlich von Strehlen in Schlesien*. *Mineral Petrogr Mitt* 48:325–372
- Schulmann K, Gayer R (2000) A model for a continental accretionary wedge developed by oblique collision: the NE Bohemian Massif. *J Geol Soc Lond* 157:401–416
- Seston R, Winchester JA, Piasecki MAJ, Crowley QG, Floyd PA (2000) A structural model for the western-central Sudetes: a deformed stack of Variscan thrust sheets. *J Geol Soc Lond* 157:1155–1167
- Shand SJ (1947) *Eruptive rocks. Their genesis, composition and relation to ore-deposits*, 3rd edn. Wiley, New York, pp 1–488
- Skácel J (1956) *Zpráva o geologickém mapování v jihovýchodní části Rychlebských hor* (in Czech). *Sbornik SLUKO Odd. A II. Olomouc*
- Skácel J (1989) *Křížení okrajového zlomu lugica a nyznerovského dislokacního pásma mezi Vapennou a Javorníkem ve Slezku*. [Crossing of the marginal fault of the Lugicum and the dislocation zone of Nyznerov between Vapenna and Javornik in Silesia (Czechoslovakia)] (in Czech with English summary). *Acta Univ Palackianae Olomucensis, Fac Rerum Nat* 95, *Geogr-Geologica* 27:31–45
- Suess FE (1912) *Die moravischen Fenster und ihre Bezirhung zum Grundgebirge des Hohen Gesenke*. *Denkschr Österr Akademie der Wissenschaften, Math-Nat* 88:541–631
- Suess FE (1926) *Intrusionstektonik und Wandertektonik im variszischen Gebirge*. Borntraeger, Berlin, 268 pp
- Szczepański J (1999) Geochemistry of the orthogneisses from the Strzelin crystalline massif (SW Poland, Fore-Sudetic Block). *Geolines* 8:68–69
- Szczepański J (2001) *Jęglowa Beds—record of polyphase deformation in the East and West Sudetes contact zone (Strzelin crystalline massif, Fore-Sudetic Block, SW Poland)* (in Polish with English summary). *Przegląd Geol* 49:63–71
- Szczepański J, Oberc-Dziedzic T (1998) Geochemistry of amphibolites from the Strzelin crystalline massif, Fore-Sudetic Block, SW Poland. *Neues Jahrb Mineral Abh* 173:23–40
- Tera F, Wasserburg G (1972) U–Th–Pb systematics in three Apollo 14 basalts and the problem of initial Pb in lunar rocks. *Earth Planet Sci Lett* 14:281–304

- Timmermann H, Parrish RR, Noble SR, Kryza R (2000) New U–Pb monazite and zircon data from the Sudetes Mountains in SW Poland: evidence for a single-cycle Variscan orogeny. *J Geol Soc Lond* 157:265–268
- van Breemen O, Aftalion M, Bowes DR, Dudek A, Misar Z, Povondra P, Vrana S (1982) Geochronological studies of the Bohemian massif, Czechoslovakia, and their significance in the evolution of Central Europe. *Trans R Soc Edinb: Earth Sci* 73:89–108
- Vavra G, Gebauer D, Schmid R, Compston W (1996) Multiple zircon growth and recrystallisation during polyphase Late Carboniferous to Triassic metamorphism in granulites of the Ivrea Zone (Southern Alps): an ion microprobe (SHRIMP) study. *Contrib Mineral Petrol* 122:337–358
- Williams IS (1998) U–Th–Pb geochronology by ion microprobe. In: McKibben MA, Shanks III WC, Ridley WI (eds) *Applications of microanalytical techniques to understanding mineralizing processes*. *Rev Econ Geol* 7:1–35
- Williams IS (2000) Response of detrital zircon and monazite, and their U–Pb isotopic systems, to regional metamorphism and host-rock partial melting, Cooma Complex, southeastern Australia. *Aust J Earth Sci* 48:557–580
- Wojnar B (1995) Structural analysis and petrology of metamorphic rocks of the southern part of the Strzelin massif (in Polish with English summary). *Acta Univ Wratislaviensis* 1633, *Prace Geol-Mineral* 46:3–74